Autonomous UAV Landing on Mobile Platforms

1st Darmesh Kumar
School of Information Technology, Engineering, Mathematics & Physics
The University of the South Pacific
Suva, Fiji
darmesh.kumar@usp.ac.fj

2nd Jai Raj
School of Information Technology, Engineering, Mathematics & Physics
The University of the South Pacific
Suva, Fiji
jai.raj@usp.ac.fj

3rd Krishna Raghuwaiya
School of Pacific Arts, Communication and Education
The University of the South Pacific
Suva, Fiji
krishna.raghuwaiya@usp.ac.fj

4th Jito Vanualailai
School of Information Technology, Engineering, Mathematics & Physics
The University of the South Pacific
Suva, Fiji
jito.vanualailai@usp.ac.fj

2021 IEEE Asia-Pacific Conference on Computer Science and Data Engineering (CSDE) | 978-1-6654-9552-3/21/$31.00 ©2021 IEEE | DOI: 10.1109/CSDE53843.2021.9718368

***Abstract*—Miniature Unmanned Aerial Vehicles, such as quadrotors, have short operational range because of limited battery capacities. As a result, they need to be charged more frequently. Mobile charging platforms are a solution to this problem. To be charged wirelessly, the Unmanned Aerial Vehicles need to communicate with the mobile charging platforms; hence the use of effective, fast and reliable technology, will be very beneficial to the quadrotors, ensuring fast charging and an effective means of transferring required data. In this paper, we consider a solution for autonomous landing of multiple quadrotors, modeled as point-masses. The multiple quadrotors, need to precisely land on mobile platforms, assumed to be equipped with wireless charging. In this article, the platforms are car-like vehicular robots, which are also modeled as point-masses in a dynamical environment, navigating in their workspace. The dynamic environment includes fixed and moving obstacles. We use a Lyapunov-based Control Scheme to propose a set of nonlinear control laws that guide the quadrotors to land safely on the moving vehicular robots which have designated targets. The effectiveness and robustness of the nonlinear acceleration control laws are verified via computer simulations.**

***Index Terms*—Lyapunov, Point-mass robots, Quadrotors, Safe landing, Stability**

I. Introduction

Robotics is overwhelmingly occupied with the developing difficulties of new and emerging avenues to reach the human frontier. With recent advancements in technology, the prospect of practical robots amongst humans is the result of collaborating, investigating, and working with humans, and together with scientific endeavours, the new generation of robots will progressively influence humans and their lives [1]. The humans fantasy of creating machines that are skilled, intelligent and autonomous are becoming a reality now, with considerable impact on many aspects of modern life, ranging from industrial manufacturing to agriculture, healthcare, transportation, emergency rescue and disaster relief, video shooting, fire-fighting, maintenance, surveillance and transportation, to name a few [2, 3, 4, 5, 6, 7, 8].

UAVs have recently gained considerable amount of interest from researchers all over the globe, with its applications in aerospace [9], military [10], demining [11] and civil [12]. UAV's typically have a short operational range and a very limited flight endurance, and with the growing use of mobile robots in almost every aspect of life, the need for easier and faster ways of landing and charging these quadrotors is also increasing. The moving mobile platforms for autonomous quadrotor landing and charging provides a solution [13, 14], hence the need to explore more state-of-the-art methods for solving such challenges. The autonomous landing of UAVs on mobile platforms present unique challenges, as the communication between the UAV and moving platform is wireless. This results in fast trajectory planning which demands a reliable and effective communication between the two vehicular system [15].

Quadrotors, amongst all the other types of UAVs, have been frequently utilised in research. Recently, Raj *et al.* in 2020 [5] used a Lyapunov-based Control Scheme (LbCS) for vertical take-off maneuvers of quadrotors that were governed by dynamical equations. They presented a new set of continuous, time-invariant nonlinear control laws that not only provided smooth trajectories from an initial position to a designated target, but also continuously minimised the roll and pitch of the quadrotor for transporting valuable and fragile payloads.

In this paper, we use the LbCS to extract control laws that govern the control and stability of mobile robots, modelled as point-mass mobile robots. The LbCS has been employed for the motion planning and control (MPC) of various robotic systems, point-mass mobile robots [4], car-like mobile robotic systems [7, 16], mobile manipulators [17], tractor-trailer systems [18, 19, 20] and quadrotors [1, 5]. The LbCS is used to the extract centralised, continuous, time-invariant acceleration-based control laws for the point-mass mobile robots. To the authors knowledge, this is the first time that the LbCS has been used to model mobile landing platforms.

A. Contributions

The main contribution of this paper are as follows:

1) The acceleration-based control laws that governs the convergence of the point-mass mobile robots on their designated mobile platforms with collision-free maneuvers.
2) A dynamic environment that includes point-mass mobile robots for autonomous landing on mobile platforms.
3) A 3-D rectangular boundary which acts as fixed obstacles where the system utilizes the vehicle-to-vehicle and vehicle-to-infrastructure communications for safe navigation.
4) The direct method of Lyapunov ensures the stability of the robotic system.

The remainder of the paper is organised as follows: in Section II, the point-mass mobile robots are modelled as quadrotors and car-like mobile robots; in Section III, the Artificial Potential Functions are defined; in Section IV, the Lyapunov function is constructed and the nonlinear acceleration control laws are extracted; in Section V, the stability analysis of the robotic system is presented; in Section VI, the simulation results are illustrated to demonstrate the effectiveness and robustness of the controllers; and Section VII finally concludes the paper with future work.

II. Robotic Model

In this section, multiple point-mass mobile robots are modelled, which represent quadrotors and mobile landing platforms.

A. UAV model

The UAVs, in 3-D workspace, are modelled as point-mass mobile robots. We give the following definition:

Definition 1. *The ith UAV modelled as a point mass, Pp_i, is a sphere of radius rp_i and centred at $(xp_i(t), yp_i(t), zp_i(t)) \in \mathbb{R}^3$ for every time $t \geqslant 0$. The ith UAV point mass is the set:*

$$Pp_i = \left\{ \begin{array}{l} (Z_1, Z_2, Z_3) \in \mathbb{R}^3 : \\ (Z_1 - xp_i)^2 + (Z_2 - yp_i)^2 + (Z_3 - zp_i)^2 \leqslant {rp_i}^2 \end{array} \right\},$$

for $i = 1, \ldots, n$.

Letting the instantaneous velocities of Pp_i to be $(\nu p_i(t), \omega p_i(t), \mu p_i(t)) = (\dot{x}p_i(t), \dot{y}p_i(t), \dot{z}p_i(t))$, the instantaneous accelerations be $(\sigma_{i1}(t), \sigma_{i2}(t), \sigma_{i3}(t)) = (\dot{\nu}p_i(t), \dot{\omega}p_i(t), \dot{\mu}p_i(t))$ and assuming the initial conditions at $t = t_0 \geqslant 0$, the kinematic model of Pp_i is:

$$\left. \begin{array}{l} \dot{x}p_i(t) = \nu p_i(t), \dot{y}p_i(t) = \omega p_i(t), \dot{z}p_i(t) = \mu p_i(t), \\ \dot{\nu}p_i(t) = \sigma_{i1}(t), \dot{\omega}p_i(t) = \sigma_{i2}(t), \dot{\mu}p_i(t) = \sigma_{i3}(t), \\ xp_{i0} := xp_i(t_0), yp_{i0} := yp_i(t_0), zp_{i0} := zp_i(t_0), \\ \nu p_{i0} = \nu p_i(t_0), \omega p_{i0} = \omega p_i(t_0), \mu p_{i0} = \mu p_i(t_0). \end{array} \right\} \quad (1)$$

B. Mobile landing platform model

The mobile landing platform, in 3-D workspace, are modelled as point-mass mobile robots. We give the following definition:

Definition 2. *The ith mobile landing platform modelled as a point mass, Pv_i, is a sphere of radius rv_i and centred at $(xv_i(t), yv_i(t), zv_i(t)) \in \mathbb{R}^3$ for $t \geqslant 0$. Precisely, it is a set:*

$$Pv_i = \left\{ \begin{array}{l} (Z_1, Z_2, Z_3) \in \mathbb{R}^3 : \\ (Z_1 - xv_i)^2 + (Z_2 - yv_i)^2 + (Z_3 - zv_i)^2 \leqslant {rv_i}^2 \end{array} \right\},$$

for $i = 1, \ldots, n$.

Letting the instantaneous velocities of Pv_i to be $(\nu v_i(t), \omega v_i(t), \mu v_i(t)) = (\dot{x}v_i(t), \dot{y}v_i(t), \dot{z}v_i(t))$, the instantaneous acceleration be $(\sigma_{i4}(t), \sigma_{i5}(t), \sigma_{i6}(t)) = (\dot{\nu}v_i(t), \dot{\omega}v_i(t), \dot{\mu}v_i(t))$ and assuming the initial conditions at $t = t_0 \geqslant 0$, the system of first-order ODE's is derived as:

$$\left. \begin{array}{l} \dot{x}v_i(t) = \nu v_i(t), \dot{y}v_i(t) = \omega v_i(t), \dot{z}v_i(t) = \mu v_i(t), \\ \dot{\nu}v_i(t) = \sigma_{i4}(t), \dot{\omega}v_i(t) = \sigma_{i5}(t), \dot{\mu}v_i(t) = \sigma_{i6}(t), \\ xv_{i0} := xv_i(t_0), yv_{i0} := yv_i(t_0), zv_{i0} := zv_i(t_0), \\ \nu v_{i0} = \nu v_i(t_0), \omega v_{i0} = \omega v_i(t_0), \mu v_{i0} = \mu v_i(t_0). \end{array} \right\} \quad (2)$$

C. Dynamic model of the team

Using systems (1) and (2), the dynamic model of the team of Pp_i and Pv_i are now given as:

$$\left. \begin{array}{l} \dot{x}p_i(t) = \nu p_i(t), \dot{y}p_i(t) = \omega p_i(t), \dot{z}p_i(t) = \mu p_i(t), \\ \dot{\nu}p_i(t) = \sigma_{i1}(t), \dot{\omega}p_i(t) = \sigma_{i2}(t), \dot{\mu}p_i(t) = \sigma_{i3}(t), \\ \dot{x}v_i(t) = \nu v_i(t), \dot{y}v_i(t) = \omega v_i(t), \dot{z}v_i(t) = \mu v_i(t), \\ \dot{\nu}v_i(t) = \sigma_{i4}(t), \dot{\omega}v_i(t) = \sigma_{i5}(t), \dot{\mu}v_i(t) = \sigma_{i6}(t) \end{array} \right\}, \quad (3)$$

for $i = 1, \ldots, n$, with the main idea to navigate Pp_i to Pv_i while ensuring collision-free maneuvers to their targets.

III. Lyapunov-based Control Scheme

In this section, we formulate the artificial potential field functions for the dynamical team that will ensure collision-free trajectories and convergence of the mobile robots to their designated targets in a $3D$ workspace.

A. Target attraction functions

The target attraction functions for Pp_i and Pv_i, for $i = 1, \ldots, n$, are formulated below.

1) Attraction function for Pp_i: The target of Pp_i is a sphere with centre (xv_i, yv_i, zv_i) and radius rp_i. To ensure that each Pp_i in the $3D$ space is attracted to its mobile target Pv_i, the target attraction function is:

$$Vp_i = \frac{1}{2}\left[\begin{array}{l} (xp_i - xv_i)^2 + (yp_i - yv_i)^2 \\ +(zp_i - (zv_i + rv_i + rp_i))^2 + {\nu p_i}^2 + {\omega p_i}^2 + {\mu p_i}^2 \end{array} \right] \quad (4)$$

for $i = 1, \ldots, n$.

2) Attraction function for Pv_i: A sphere with centre $(\tau_{i1}, \tau_{i2}, \tau_{i3})$ and radius $r\tau_i$ is modelled as a stationary target for Pv_i. To ensure that each Pv_i is attracted to its defined target, the target attraction function is:

$$Vv_i = \frac{1}{2}\left[\begin{array}{l} (xv_i - \tau_{i1})^2 + (yv_i - \tau_{i2})^2 + (zv_i - \tau_{i3})^2 \\ +{\nu v_i}^2 + {\omega v_i}^2 + {\mu v_i}^2 \end{array} \right], \quad (5)$$

for $i = 1, \ldots, n$.

B. Auxiliary functions

1) Auxiliary function for Pp_i: To guarantee the convergence of each Pp_i to its designated target and ensure that the non- linear controllers vanish at the target, the auxiliary function is:

$$Gp_i = \frac{1}{2}\left[\begin{array}{l} (xp_i - xv_i)^2 + (yp_i - yv_i)^2 \\ +(zp_i - (zv_i + rv_i + rp_i))^2 \end{array} \right], \quad (6)$$

for $i = 1, \ldots, n$.

2) Auxiliary function for Pv_i: To guarantee the convergence of each Pv_i to its designated fixed target and ensure that the non- linear controllers vanish at the target, the auxiliary function is:

$$Gv_i = \frac{1}{2}\left[(xv_i - \tau_{i1})^2 + (yv_i - \tau_{i2})^2 + (zv_i - \tau_{i3})^2\right], \quad (7)$$

for $i = 1, \ldots, n$.

C. Obstacle Avoidance Functions

In this section, we design functions that act as obstacle avoidance functions for Pp_i and Pv_i.

1) Workspace Boundary Limitations: We consider a 3-dimensional workspace of dimension $\eta_1 \times \eta_2 \times \eta_3$. The boundary walls are treated as fixed obstacles which the mobile robots need to avoid.Thus we construct the obstacle avoidance functions.

a) Boundary avoidance by the UAV model: For each Pp_i to avoid the workspace boundaries, the following obstacle avoidance functions are designed:

$$\left.\begin{array}{l} Wp_{i1} = xp_i - rp_i,\ Wp_{i4} = \eta_1 - (xp_i + rp_i),\\ Wp_{i2} = yp_i - rp_i,\ Wp_{i5} = \eta_2 - (yp_i + rp_i),\\ Wp_{i3} = zp_i - rp_i,\ Wp_{i6} = \eta_3 - (zp_i + rp_i), \end{array}\right\} \quad (8)$$

for $i = 1, \ldots, n$.

b) Boundary avoidance by the mobile landing platform model: For each Pv_i to avoid the workspace boundaries, the following obstacle avoidance functions are designed:

$$\left.\begin{array}{l} Wv_{i1} = xv_i - rv_i,\ Wv_{i4} = \eta_1 - (xv_i + rv_i),\\ Wv_{i2} = yv_i - rv_i,\ Wv_{i5} = \eta_2 - (yv_i + rv_i),\\ Wv_{i3} = zv_i - rv_i,\ Wv_{i6} = \eta_3 - (zv_i + rv_i), \end{array}\right\} \quad (9)$$

for $i = 1, \ldots, n$.

2) Fixed obstacles: Let us consider $q \in \mathbb{N}$ spherically shaped obstacles with center (o_{r1}, o_{r2}, o_{r3}) and radius ro_r. For Pp_i and Pv_i to avoid these fixed obstacles, obstacle avoidance functions are designed.

a) Fixed obstacle avoidance by the UAV model: For each Pp_i to avoid the qth fixed spherical obstacle, the following obstacle avoidance function is designed:

$$Fp_{ir} = \frac{1}{2}\begin{bmatrix}(xp_i - o_{r1})^2 + (yp_i - o_{r2})^2 + (zp_i - o_{r3})^2\\ -(rp_i + ro_r)^2\end{bmatrix}, \quad (10)$$

for $r = 1, ..., q$ and $i = 1, \ldots, n$.

b) Fixed obstacle avoidance by the mobile landing platform model: For each Pv_i to avoid the qth fixed spherical obstacle, the following obstacle avoidance function is designed:

$$Fv_{ir} = \frac{1}{2}\begin{bmatrix}(xv_i - o_{r1})^2 + (yv_i - o_{r2})^2 + (zv_i - o_{r3})^2\\ -(rv_i + ro_r)^2\end{bmatrix}, \quad (11)$$

for $r = 1, ..., q$ and $i = 1, \ldots, n$.

3) Moving Obstacles: Each mobile robot becomes a moving obstacle for all the other mobile robots in the workspace. There are moving obstacles in the form of the point-mass mobile robots which represents the quadrotor and the vehicular mobile robots. Obstacle avoidance functions are designed to ensure the mobile robots avoid each other.

a) Moving obstacle avoidance by the UAV model: For the ith mobile robot to avoid the jth mobile robot, we consider the following obstacle avoidance function:

$$Mp_{ij} = \frac{1}{2}\begin{bmatrix}(xp_i - xp_j)^2 + (yp_i - yp_j)^2 + (zp_i - zp_j)^2\\ -(2rp_i)^2\end{bmatrix}, \quad (12)$$

where $i, j = 1, \ldots, n$ and $j \neq i$.

b) Moving obstacle avoidance by the mobile landing platform model: For the ith mobile landing platform to avoid the jth mobile landing platform, we consider the following obstacle avoidance function:

$$Mv_{ij} = \frac{1}{2}\begin{bmatrix}(xv_i - xv_j)^2 + (yv_i - yv_j)^2 + (zv_i - zv_j)^2\\ -(2\,rv_i)^2\end{bmatrix}, \quad (13)$$

where $i, j = 1, \ldots, n$ and $j \neq i$.

IV. Design of the Nonlinear Control Laws

In this section, the nonlinear control laws governing system (3) will be designed in accordance to the LbCS. First we construct the Lyapunov function and then extract the control laws that will govern the motion of Pp_i and Pv_i, for $i = 1, \ldots, n$.

A. Lyapunov Function

The Lyapunov function, also known as the total potentials, is a sum of all attractive and repulsive potential functions. The obstacle avoidance functions, when suitably combined with the appropriate *tuning parameters*, form the repulsive potential field functions. We begin by defining the following tuning parameters:

(i) $\alpha_{ir} > 0, r = 1, ..., q$, for Pp_i to avoid the rth fixed spherical obstacle;
(ii) $\varsigma_{ir} > 0, r = 1, ..., q$, for Pv_i to avoid the rth fixed spherical obstacle;
(iii) $\beta_{is} > 0, s = 1, ..., 6$, for Pp_i to avoid the sth boundary wall of the workspace;
(iv) $\gamma_{is} > 0, s = 1, ..., 6$, for Pv_i to avoid the sth boundary wall of the workspace;
(v) $\zeta_{ij} > 0,\ j = 1, \ldots, n,\ j \neq i$, for Pp_i to avoid the jth mobile robot;
(vi) $\psi_{ij} > 0,\ j = 1, \ldots, n,\ j \neq i$, for Pv_i to avoid the jth mobile landing platform,

for $i = 1, \ldots, n$. The tentative Lyapunov function for system (3) is defined as follows:

$$L(\mathbf{x}) = \sum_{i=1}^{n}\begin{bmatrix} Vp_i(\mathbf{x}) + Vv_i(\mathbf{x}) + Gp_i(\mathbf{x})\displaystyle\sum_{s=1}^{6}\frac{\beta_{is}}{Wp_{is}(\mathbf{x})}\\ +Gp_i(\mathbf{x})\left(\displaystyle\sum_{\substack{j=1\\ i\neq j}}^{n}\frac{\zeta_{ij}}{Mp_{ij}(\mathbf{x})} + \sum_{r=1}^{q}\frac{\alpha_{ir}}{Fp_{ir}(\mathbf{x})}\right)\\ +Gv_i(\mathbf{x})\displaystyle\sum_{\substack{j=1\\ i\neq j}}^{n}\frac{\psi_{ij}}{Mv_{ij}(\mathbf{x})}\\ +Gv_i(\mathbf{x})\left(\displaystyle\sum_{r=1}^{q}\frac{\varsigma_{ir}}{Fv_{ir}(\mathbf{x})} + \sum_{s=1}^{6}\frac{\gamma_{is}}{Wv_{is}(\mathbf{x})}\right)\end{bmatrix}, \quad (14)$$

which is positive over the domain.

B. Nonlinear Acceleration Controllers

The differentiation of various components of $L(\mathbf{x})$ along t is used to extract the kinodynamic system's control laws.The following are the components of the control inputs:

$$f_{i1}=\left(1+\sum_{r=1}^{q}\frac{\alpha_{ir}}{Fp_{ir}}+\sum_{s=1}^{6}\frac{\beta_{is}}{Wp_{is}}+\sum_{\substack{j=1\\i\neq j}}^{n}\frac{\zeta_{ij}}{Mp_{ij}}\right)(xp_i-xv_i)$$
$$-Gp_i\left(\begin{array}{c}\sum_{r=1}^{q}\frac{\alpha_{ir}}{(Fp_{ir})^2}(xp_i-o_{r1})+\frac{\beta_{i1}}{(Wp_{i1})^2}\\+2\sum_{\substack{j=1\\i\neq j}}^{n}\frac{\zeta_{ij}}{(Mp_{ij})^2}(xp_i-xp_j)-\frac{\beta_{i4}}{(Wp_{i4})^2}\end{array}\right),$$

$$f_{i2}=\left(1+\sum_{r=1}^{q}\frac{\alpha_{ir}}{Fp_{ir}}+\sum_{s=1}^{6}\frac{\beta_{is}}{Wp_{is}}+\sum_{\substack{j=1\\i\neq j}}^{n}\frac{\zeta_{ij}}{Mp_{ij}}\right)(yp_i-yv_i)$$
$$-Gp_i\left(\begin{array}{c}\sum_{r=1}^{q}\frac{\alpha_{ir}}{(Fp_{ir})^2}(yp_i-o_{r2})+\frac{\beta_{i2}}{(Wp_{i2})^2}\\+2\sum_{\substack{j=1\\i\neq j}}^{n}\frac{\zeta_{ij}}{(Mp_{ij})^2}(yp_i-yp_j)-\frac{\beta_{i5}}{(Wp_{i5})^2}\end{array}\right),$$

$$f_{i3}=\left(1+\sum_{r=1}^{q}\frac{\alpha_{ir}}{Fp_{ir}}+\sum_{s=1}^{6}\frac{\beta_{is}}{Wp_{is}}\right)(zp_i-zv_i-rv_i-rp_i)$$
$$-Gp_i\left(\begin{array}{c}\sum_{r=1}^{q}\frac{\alpha_{ir}}{(Fp_{ir})^2}(zp_i-o_{r3})+\frac{\beta_{i3}}{(Wp_{i3})^2}\\+2\sum_{\substack{j=1\\i\neq j}}^{n}\frac{\zeta_{ij}}{(Mp_{ij})^2}(zp_i-zp_j)-\frac{\beta_{i6}}{(Wp_{i6})^2}\end{array}\right)$$
$$+\sum_{\substack{j=1\\i\neq j}}^{n}\frac{\zeta_{ij}}{Mp_{ij}}(zp_i-zv_i-rv_i-rp_i),$$

$$f_{i4}=\left(1+\sum_{r=1}^{q}\frac{\varsigma_{ir}}{Fv_{ir}}+\sum_{s=1}^{6}\frac{\gamma_{is}}{Wv_{is}}+\sum_{\substack{j=1\\i\neq j}}^{n}\frac{\psi_{ij}}{Mv_{ij}}\right)(xv_i-\tau_{i1})$$
$$-\left(1+\sum_{r=1}^{q}\frac{\alpha_{ir}}{Fp_{ir}}+\sum_{s=1}^{6}\frac{\beta_{is}}{Wp_{is}}+\sum_{\substack{j=1\\i\neq j}}^{n}\frac{\zeta_{ij}}{Mp_{ij}}\right)(xp_i-xv_i)$$
$$-Gv_i\left(\begin{array}{c}\sum_{r=1}^{q}\frac{\varsigma_{ir}}{(Fv_{ir})^2}(xv_i-o_{r1})+\frac{\gamma_{i1}}{(Wv_{i1})^2}\\+2\sum_{\substack{j=1\\i\neq j}}^{n}\frac{\psi_{ij}}{(Mv_{ij})^2}(xv_i-xv_j)-\frac{\gamma_{i4}}{(Wv_{i4})^2}\end{array}\right),$$

$$f_{i5}=\left(1+\sum_{r=1}^{q}\frac{\varsigma_{ir}}{Fv_{ir}}+\sum_{s=1}^{6}\frac{\gamma_{is}}{Wv_{is}}+\sum_{\substack{j=1\\i\neq j}}^{n}\frac{\psi_{ij}}{Mv_{ij}}\right)(yv_i-\tau_{i2})$$
$$-\left(1+\sum_{r=1}^{q}\frac{\alpha_{ir}}{Fp_{ir}}+\sum_{s=1}^{6}\frac{\beta_{is}}{Wp_{is}}+\sum_{\substack{j=1\\i\neq j}}^{n}\frac{\zeta_{ij}}{Mp_{ij}}\right)(yp_i-yv_i)$$
$$-Gv_i\left(\begin{array}{c}\sum_{r=1}^{q}\frac{\varsigma_{ir}}{(Fv_{ir})^2}(yv_i-o_{r2})+\frac{\gamma_{i2}}{(Wv_{i2})^2}\\+2\sum_{\substack{j=1\\i\neq j}}^{n}\frac{\psi_{ij}}{(Mv_{ij})^2}(yv_i-yv_j)-\frac{\gamma_{i5}}{(Wv_{i5})^2}\end{array}\right),$$

$$f_{i6}=\left(\sum_{r=1}^{q}\frac{\varsigma_{ir}}{Fv_{ir}}+\sum_{s=1}^{6}\frac{\gamma_{is}}{Wv_{is}}+\sum_{\substack{j=1\\i\neq j}}^{n}\frac{\psi_{ij}}{Mv_{ij}}\right)(zv_i-\tau_{i3})$$
$$-\left(\sum_{r=1}^{q}\frac{\alpha_{ir}}{Fp_{ir}}+\sum_{s=1}^{6}\frac{\beta_{is}}{Wp_{is}}+\sum_{\substack{j=1\\i\neq j}}^{n}\frac{\zeta_{ij}}{Mp_{ij}}\right)\begin{pmatrix}zp_i-zv_i\\-rv_i-rp_i\end{pmatrix}$$
$$-Gv_i\left(\begin{array}{c}\sum_{r=1}^{q}\frac{\varsigma_{ir}}{(Fv_{ir})^2}(zv_i-o_{r3})+\frac{\gamma_{i3}}{(Wv_{i3})^2}\\+2\sum_{\substack{j=1\\i\neq j}}^{n}\frac{\psi_{ij}}{(Mv_{ij})^2}(zv_i-zv_j)-\frac{\gamma_{i6}}{(Wv_{i6})^2}\end{array}\right)$$
$$+(zv_i-\tau_{i3})-(zp_i-zv_i-rv_i-rp_i).$$

Choosing the convergence parameters to be $\delta_{i1},\delta_{i2},\delta_{i3},\delta_{i4},\delta_{i5},\delta_{i6}>0$, we get the following controllers:

$$\left.\begin{array}{l}\sigma_{i1}=-(\delta_{i1}\nu p_i+f_{i1}),\sigma_{i2}=-(\delta_{i2}\omega p_i+f_{i2}),\\\sigma_{i3}=-(\delta_{i3}\mu p_i+f_{i3}),\sigma_{i4}=-(\delta_{i4}\nu v_i+f_{i4}),\\\sigma_{i5}=-(\delta_{i5}\omega v_i+f_{i5}),\sigma_{i6}=-(\delta_{i6}\mu v_i+f_{i6}),\end{array}\right\}\qquad(15)$$

for $i=1,\ldots,n$.

V. Stability Analysis

Using the notations $\mathbf{x}_{e_i}:=(\tau_{i1},\tau_{i2},\tau_{i3})\in\mathbb{R}^3$ and $\mathbf{x}_e:=(\mathbf{x}_{e_1},\ldots,\mathbf{x}_{e_n})\in\mathbb{R}^{3n}$, we state the following theorem:

Theorem 5.1: A stable equilibrium point of system (3) is $\mathbf{x}_e\in\mathbb{D}(L(\mathbf{x}))$.

Proof. Since the Lyapunov function $L(\mathbf{x})$ of system (3) is defined, continuous and positive over the domain $\mathbb{D}(L(\mathbf{x}))=\{\mathbf{x}\in\mathbb{R}^{3n}: Wp_{is}(\mathbf{x})>0,\ s=1,...,6;\ Wv_{is}(\mathbf{x})>0,\ s=1,...,6;\ Fp_{ir}(\mathbf{x})>0,\ r=1,...,q;\ Fv_{ir}(\mathbf{x})>0,\ r=1,...,q;\ Mp_{ij}(\mathbf{x})>0,\ j\neq i;\ Mv_{ij}(\mathbf{x})>0,\ j\neq i\}$ for $i=1,...,n$, it can easily be verified that $L(\mathbf{x})$ satisfies the following properties:

1) $L(\mathbf{x})$ is continuous in the region $\mathbb{D}$ in the neighborhood of the point $\mathbf{x}_e$ of system (3);
2) $L(\mathbf{x}_e)=0$;
3) $L(\mathbf{x})>0\ \ \forall\mathbf{x}\in\mathbb{D}(L(\mathbf{x}))/\mathbf{x}_e$.

Then, along a solution of system (3), we have:

$$\dot{L}_{(3)}(\mathbf{x})=\sum_{i=1}^{n}\begin{bmatrix}f_{i1}\dot{x}p_i+f_{i2}\dot{y}p_i+f_{i3}\dot{z}p_i\\+f_{i4}\dot{x}v_i+f_{i5}\dot{y}v_i+f_{i6}\dot{z}v_i\\+\sigma_{i1}\dot{x}p_i+\sigma_{i2}\dot{y}p_i+\sigma_{i3}dotzp_i\\+\sigma_{i4}\dot{x}v_i+\sigma_{i5}\dot{y}v_i+\sigma_{i6}\dot{z}v_i\end{bmatrix}\qquad(16)$$

Using (15), we have the following time derivative of $L(\mathbf{x})$ which is the semi-negative definite function for system (3):

$$\dot{L}_{(3)}(\mathbf{x})=-\sum_{i=1}^{n}\begin{bmatrix}\delta_{i1}\nu p_i{}^2+\delta_{i2}\omega p_i{}^2+\delta_{i3}\mu p_i{}^2\\+\delta_{i4}\nu v_i{}^2+\delta_{i5}\omega v_i{}^2+\delta_{i6}\mu v_i{}^2\end{bmatrix}\leqslant 0.$$

Therefore, $\dot{L}_{(3)}(\mathbf{x})\leq 0\ \forall\mathbf{x}\in\mathbb{D}(L(\mathbf{x}))$ and $\dot{L}_{(3)}(\mathbf{x}_e)=0$. Moreover $L(\mathbf{x})\in C^1(\mathbb{D}(L(\mathbf{x})))$, hence, for system (3), $L(\mathbf{x})$ is classified as its Lyapunov function and $\mathbf{x}_e$ is a stable equilibrium point.

VI. Simulation Results

This section provides an example of the navigation control of $n = 2$ point-mass model of UAVs and mobile landing platforms in an environment cluttered with spherical obstacles. Each UAV point-mass navigates and lands on its assigned mobile landing platform. After smooth landing, the combined system of the UAV point-masses and the mobile landing platforms converge together to their designated target, while ensuring obstacle avoidance. In order to avoid the fixed obstacles, the combined systems needed to move either right or left, while ensuring collision avoidance between the different combined systems and thus, guaranteeing the stability of the landed UAV modelled point-masses. The initial conditions, constraints and the parameters used in the simulations are provided in Table I.

The trajectories at different viewing angles are shown in Figure 1. Figures 1(a), 1(b) and 1(c) demonstrate the default, bird's-eye and front views of the trajectories of Pp_i and Pv_i for $i = 1, 2$, at times $t = 0, 40, 410, 2200$, respectively. Figure 2(a) shows the behaviour of the Lyapunov function while its time derivative is shown in Figure 2(b) along the trajectories of the system. The stability results obtained from the Lyapunov function are verified numerically.

TABLE I
THE PARAMETERS USED IN THE NUMERICAL SIMULATION WITH $n = 2$ AND $q = 2$.

Description	Value
Initial state of the point-mass mobile robots	
Workspace	$\eta_1 = 210$, $\eta_2 = 150$, $\eta_3 = 120$
Initial position, radius of Pp_i	$(xp_1, yp_1, zp_1) = (30, 20, 100)$, $rp_1 = 1$
	$(xp_2, yp_2, zp_2) = (10, 100, 100)$, $rp_2 = 1$
Initial position, radius of Pv_i	$(xv_1, yv_1, zv_1) = (30, 20, 10)$, $rv_1 = 4$
	$(xv_2, yv_2, zv_2) = (20, 100, 10)$, $rv_2 = 4$
Spherical obstacles	$(o_{11}, o_{12}, o_{13}) = (150, 100, 21)$, $ro_1 = 20$
- position, radius	$(o_{21}, o_{22}, o_{23}) = (80, 80, 21)$, $ro_2 = 20$
Constraints	
Target centre, radius	$(\tau_{11}, \tau_{12}, \tau_{13}) = (200, 130, 10)$, $r\tau_1 = 3$
	$(\tau_{21}, \tau_{22}, \tau_{23}) = (200, 40, 10)$, $r\tau_2 = 3$
Control and convergence parameters	
Avoidance of workspace by Pp_i	$\beta_{is} = 10$ for $i = 1, 2$, $s = 1, \ldots, 6$
Avoidance of workspace by Pv_i	$\gamma_{is} = 10$ for $i = 1, 2$, $s = 1, \ldots, 6$
Avoidance of spherical obstacle by Pp_i	$\alpha_{ir} = 100$, for $i = 1, 2$, $r = 1, 2$
Avoidance of spherical obstacle by Pv_i	$\varsigma_{ir} = 100$, for $i = 1, 2$, $r = 1, 2$
Inter individual collision avoidance by Pp_i	$\zeta_{ij} = 5$ for $i = j = 1, 2$, $j \neq i$
Inter individual collision avoidance by Pv_i	$\psi_{ij} = 5$ for $i = j = 1, 2$, $j \neq i$
Convergence of Pp_i to Pv_i	$\delta_{i1} = \delta_{i2} = \delta_{i3} = 20$, for $i = 1, 2$
Convergence of Pv_i to target	$\delta_{i4} = \delta_{i5} = 10^3$, $\delta_{i6} = 10^6$, for $i = 1, 2$

VII. Conclusion

The motion planning and control of robotic systems is a very intriguing problem with researchers all over the globe devising advanced methods of control, with advancements in technology, following the growing need in the military and civilian sectors. The novelty of the paper lies in the use of the LbCS, which has been applied to derive a set of robust, unique continuous time-invariant acceleration-based control laws for the MPC of UAVs modelled as point-masses for autonomous, precise and safe landing on mobile platforms. The dynamic environment under consideration included fixed and moving obstacles which were avoided by the UAV and the mobile landing platforms. The direct method of Lyapunov is used to prove the stability of the dynamic model. Computer simulations were used to illustrate the effectiveness and robustness of the control scheme.

This work paves the manner for several future headings. Autonomous landing of quadrotors on mobile landing platforms in the presence of obstacles would be a new addition to the MPC problem.

References

[1] J. Vanualailai, J. Raj, and K. Raghuwaiya, "Autonomous quadrotor maneuvers in a 3d complex environment," in *Advances in Computer, Communication and Computational Sciences*. Springer, 2021, pp. 221–231.

[2] E. Kalantari, M. Z. Shakir, H. Yanikomeroglu, and A. Yongacoglu, "Backhaul-aware robust 3d drone placement in 5g+ wireless networks," in *2017 IEEE international conference on communications workshops (ICC workshops)*. IEEE, 2017, pp. 109–114.

[3] K. S. Raghuwaiya, B. Sharma, and J. Vanualailai, "Leader-follower based locally rigid formation control," *Journal of Advanced Transportation*, vol. 2018, pp. 1–14, 02 2018.

[4] J. Raj, K. S. Raghuwaiya, and J. Vanualailai, "Collision avoidance of 3d rectangular planes by multiple cooperating autonomous agents," *Journal of Advanced Transportation*, vol. 2020, pp. 1 – 13, 10 2020.

[5] J. Raj, K. Raghuwaiya, and J. Vanualailai, "Novel lyapunov-based autonomous controllers for quadrotors," *IEEE Access*, vol. 8, no. 1, pp. 47 393 – 47 406, 2020.

[6] H. Ríos, R. Falcón, O. A. González, and A. Dzul, "Continuous sliding-mode control strategies for quadrotor robust tracking: Real-time application," *IEEE Transactions on Industrial Electronics*, vol. 66, no. 2, pp. 1264–1272, Feb 2019.

[7] B. Sharma, J. Raj, and J. Vanualailai, "Navigation of carlike robots in an extended dynamic environment with swarm avoidance," *International Journal of Robust and Nonlinear Control*, vol. 28, no. 2, pp. 678–698, 2018.

[8] V. Chand, A. Prasad, K. Chaudhary, B. Sharma, and S. Chand, "A face-off-classical and heuristic-based path planning approaches," in *2020 IEEE Asia-Pacific Conference on Computer Science and Data Engineering (CSDE)*. IEEE, 2020, pp. 1–6.

[9] R. Materna, "Highlights from aerospace industry report 2012: Facts, figures and outlook for the aviation and aerospace manufacturing industry," *Aerospace Industries Association of America Inc.: Arlington, VA, USA*, 2012.

[10] I. Jang, J. Jeong, H.-S. Shin, S. Kim, A. Tsourdos, and J. Suk, "Cooperative control for a flight array of uavs and

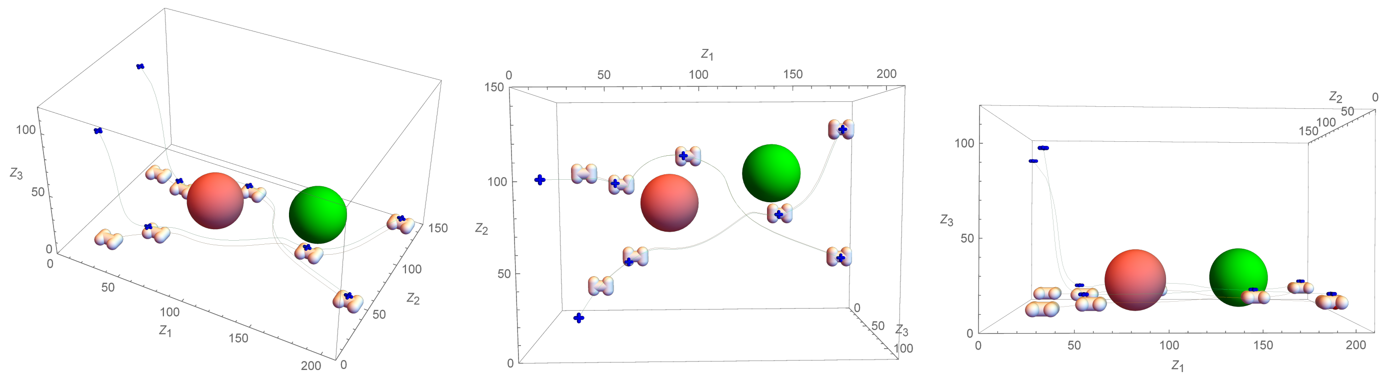

(a) Default 3D motion view. (b) Top 3D motion view. (c) Front 3D motion view.

Fig. 1. The different viewpoints of Pp_i and Pv_i, for $i = 1, 2$, in its motion to its target while avoiding spherical obstacles.

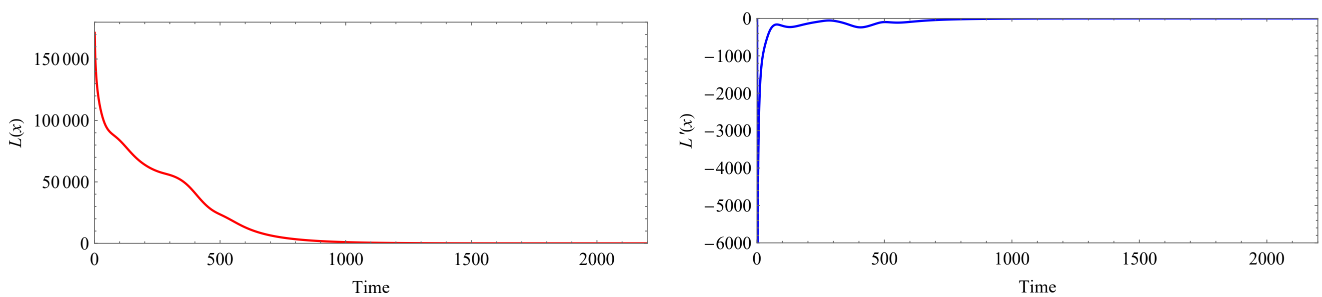

(a) Lyapunov function. (b) Lyapunov function time derivative.

Fig. 2. The behaviour of the Lyapunov function and its time derivative for system (3).

an application in radar jamming," *IFAC-PapersOnLine*, vol. 50, no. 1, pp. 8011–8018, 2017.

[11] F. J. Pereda, H. G. de Marina, Juan Francisco Jiménez, and J. M. Giron-Sierra, "Sea demining with autonomous marine surface vehicles," in *2010 IEEE Safety Security and Rescue Robotics*, 2010, pp. 1–6.

[12] R. Avtar, S. A. Suab, A. P. Yunus, P. Kumar, P. K. Srivastava, M. Ramaiah, and C. A. Juan, *Applications of UAVs in Plantation Health and Area Management in Malaysia*. Cham: Springer International Publishing, 2020, pp. 85–100.

[13] D. Lee, T. Ryan, and H. J. Kim, "Autonomous landing of a vtol uav on a moving platform using image-based visual servoing," in *2012 IEEE international conference on robotics and automation*. IEEE, 2012, pp. 971–976.

[14] G. Zhang, H. Kuang, and X. Liu, "Fast trajectory optimization for quadrotor landing on a moving platform," in *2020 International Conference on Unmanned Aircraft Systems (ICUAS)*, 2020, pp. 238–246.

[15] A. Paris, B. T. Lopez, and J. P. How, "Dynamic landing of an autonomous quadrotor on a moving platform in turbulent wind conditions," in *2020 IEEE International Conference on Robotics and Automation (ICRA)*, 2020, pp. 9577–9583.

[16] J. Raj, K. Raghuwaiya, J. Vanualailai, and B. Sharma, "Navigation of car-like robots in three-dimensional space," in *2018 5th Asia-Pacific World Congress on Computer Science and Engineering (APWC on CSE)*. IEEE, 2018, pp. 271–275.

[17] A. Prasad, B. Sharma, J. Vanualailai, and S. Kumar, "Motion control of an articulated mobile manipulator in 3d using the lyapunov-based control scheme," *International Journal of Control*, vol. 0, no. 0, pp. 1–15, 2021.

[18] A. Prasad, B. N. Sharma, J. Vanualailai, and S. A. Kumar, "A geometric approach to target convergence and obstacle avoidance of a nonstandard tractor-trailer robot," *International Journal of Robust and Nonlinear Control*, vol. 30, pp. 4924–4943, 2020.

[19] J. Raj, K. S. Raghuwaiya, S. Singh, B. Sharma, and J. Vanualailai, "Swarming intelligence of 1-trailer systems," in *Advanced Computer and Communication Engineering Technology*, H. A. Sulaiman, M. A. Othman, M. F. I. Othman, Y. A. Rahim, and N. C. Pee, Eds. Cham: Springer International Publishing, 2016, pp. 251–264.

[20] J. Raj, K. Raghuwaiya, B. Sharma, and J. Vanualailai, "Motion control of a flock of 1-trailer robots with swarm avoidance," *Robotica*, pp. 1–26, 2021.